

Fine, I'll Merge It Myself: A Multi-Fidelity Framework for Automated Model Merging

Guinan Su¹ Jonas Geiping^{1,2,3}

¹Max Planck Institute for Intelligent Systems, ²ELLIS Institute Tübingen, ³Tübingen AI Center

Abstract

Reasoning capabilities represent a critical frontier for large language models (LLMs), but developing them requires extensive proprietary datasets and computational resources. One way to efficiently supplement capabilities with is by model merging, which offers a promising alternative by combining multiple models without retraining. However, current merging approaches rely on manually-designed strategies for merging hyperparameters, limiting the exploration of potential model combinations and requiring significant human effort. We propose an Automated Model Merging Framework that enables fine-grained exploration of merging strategies while reducing costs through multi-fidelity approximations. We support both single and multi-objective optimization and introduce two novel search spaces: layer-wise fusion (LFS) and depth-wise integration (DIS). Evaluating across a number of benchmarks, we find that the search autonomously finds 1) Merges that further boost single-objective performance, even on tasks the model has already been finetuned on, and 2) Merges that optimize multi-objective frontiers across tasks. Effective merges are found with limited compute, e.g. within less than 500 search steps. The code is available at.¹

1. Introduction

Recent advancements in large-scale pre-trained models like GPT-4 (OpenAI et al., 2023), LLaMA (Touvron et al., 2023), DALL-E (Ramesh et al., 2021), and Imagen (Saharia et al., 2022) have demonstrated remarkable capabilities across diverse domains. Within Large Language Models (LLMs), specialized models have emerged excelling in specific tasks such as instruction following (Xu et al., 2023; Jiang et al., 2023; Bi et al., 2024), code generation (Luo

¹<https://github.com/Guinan-Su/auto-merge-llm>

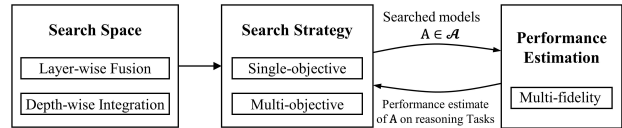


Figure 1. Overview of our Proposed Merging Framework: Search space: layer-wise fusion (LFS) and depth-wise integration (DIS), search strategy optimization with single/multi-objective approaches, and multi-fidelity performance estimation

et al., 2023b; Guo et al., 2024; Zhu et al., 2024), and mathematical problem-solving (Luo et al., 2023a). However, developing models with comprehensive reasoning capabilities remains challenging. A straightforward solution would be to combine training data from specialized domains for retraining or finetuning. However, this data-centric approach faces practical limitations: it requires substantial resources, and many training datasets remain proprietary or restricted. Researchers have turned to model-centric approaches that enhance capabilities by leveraging existing pre-trained models without requiring training or data access.

Model merging has emerged as a promising solution in this space. Beginning with simple weight averaging for models sharing initialization (Utans, 1996), more advanced parameter-based techniques were subsequently developed. Parameter-based methods like Task Arithmetic (Ilharco et al., 2022) and SLERP (White, 2016) advanced the field through parameter difference computation and spherical interpolation. Recent sparsity-based approaches like TIES-Merging (Yadav et al., 2024) and DARE (Yu et al., 2024) leverage neural network over-parametrization, using magnitude-based selection and rescaling to further improve merging effectiveness. However, these model merging methods rely on manually-tuned hyperparameters, applied uniformly across the entire model. This approach relies heavily on manual hyperparameter tuning, and its coarse granularity makes finding optimal solutions challenging. In this paper, we propose a **cost-efficient automated framework** for enhancing reasoning through model merging. Our approach

leverages Multi-Fidelity Optimization (MFO) (Peherstorfer et al., 2018) to optimize the merging process through low-fidelity approximations, reducing computational cost. We support both single and multi-objective optimization and introduce layer-wise and depth-wise search spaces for finer-grained merging. Our key contributions include:

- We propose an automated model merging framework that enhances both single and multi-objective reasoning capabilities while reducing computational costs through multi-level fidelity optimization.
- We introduce two novel search spaces: Layer-wise Fusion Space (LFS) for fine-grained layer merging and Depth-wise Integration Space (DIS) for optimizing inference pathways, enabling comprehensive model integration strategies.
- We demonstrated efficient optimization across different scenarios: in mathematical reasoning using LFS, only 17% of trials required the full search budget within 500 trials; in general reasoning using DIS, only 18.6% of trials required the full budget within 1000 trials.
- We achieve significant performance gains, including a 6.86% average improvement in multi-objective scenarios and a 4.24% improvement on the challenging GSM8K task, with consistent effectiveness across various reasoning benchmarks.

2. Related Work

2.1. Model Merging

Model merging has emerged as an efficient approach to enhance model capabilities without additional training data or extensive computation. The field has evolved from simple weighted parameter averaging to increasingly sophisticated methods. Early methods employed weighted parameter averaging (Utans, 1996) for models fine-tuned from a shared base model. Despite being simple to implement, these approaches often yielded suboptimal results. More advanced parameter-based techniques like Task Arithmetic (Ilharco et al., 2022) and SLERP (White, 2016) introduced parameter differences computation and spherical interpolation respectively. Later developments leveraged neural network sparsity, with TIES-Merging (Yadav et al., 2024) selectively retaining parameters based on magnitude while addressing sign conflicts, and DARE (Yu et al., 2024) combining magnitude-based sparsification with parameter rescaling. Recent advances include Evolutionary model merging (Akiba et al., 2024), which optimizes merging coefficients through evolutionary search. In this study, our framework also focuses on automatic model merging, while we propose a novel framework that leverages Multi-fidelity optimization

(Peherstorfer et al., 2018) based on SMAC (Lindauer et al., 2022), optimizing merging recipes through layer fusion and pathway optimization for enhanced reasoning capabilities.

2.2. Hyperparameter Optimization

Bayesian Optimization has demonstrated remarkable success across various applications, from achieving state-of-the-art results on CIFAR-10 (Snoek et al., 2012) to winning multiple datasets in the 2016 AutoML challenge (Mendoza et al., 2016). Although Gaussian processes remain the predominant probabilistic model in Bayesian optimization due to their well-calibrated uncertainty estimates, they face limitations in scalability, flexibility, and robustness. Alternative models such as random forests (Hutter et al., 2011) and Bayesian neural networks (Snoek et al., 2015; Springenberg et al., 2016; Perrone et al., 2017) offer better scalability for high-dimensional spaces.

Hyperband is one of the most widely-used multi-fidelity optimization (Peherstorfer et al., 2018) methods. It dynamically allocates resources across random configurations, while applying successive halving (Jamieson & Talwalkar, 2016) to eliminate poor options early. Although this method demonstrates superior performance and scalability compared to traditional Bayesian optimization, its random sampling strategy fails to leverage information from previous evaluations, potentially limiting its performance.

Our optimizer builds upon SMAC (Lindauer et al., 2022), combining Hyperband (HB) and Bayesian Optimization (BO) to harness both efficient resource allocation and learning capabilities through surrogate modeling for effective multi-fidelity optimization. We integrate this approach into our framework to enable effective and efficient searching.

3. Method

3.1. Overview

To define a hyperparameter optimization pipeline for model merging, we need three parts, a search space, a target objective, and a search strategy. Our framework introduces two model merging search spaces: A Layer-wise Fusion Search Space (LFS) and a Depth-wise Integration Search Space (DIS). LFS provides fine-grained layer-wise merging, merging weights at corresponding layers from multiple models according to an optimal merge operation. However, finetuned models may not always contain corresponding layers that can be merged, even if they contain complementary information. The DIS space addresses this limitation by maintaining individual layer weights while optimizing their sequential arrangement, enabling the discovery of optimal inter-layer relationships, e.g. by picking up both copies of a corresponding layer from a model pair and placing both in an optimal order in the merged model. To accelerate the

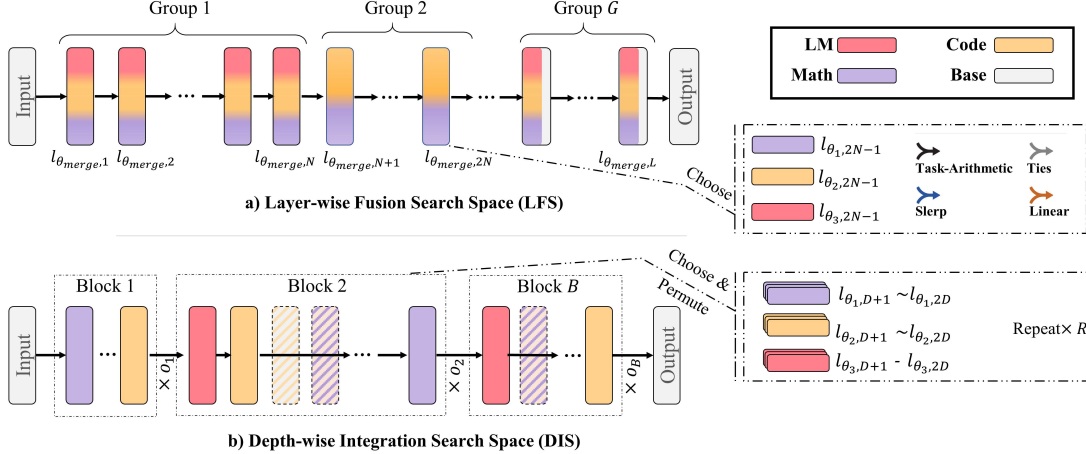


Figure 2. Illustrations of two merging search spaces: (a) Layer-wise Fusion Search (LFS), which merges layers across layer groups with different methods and hyper-parameters, and (b) Depth-wise Integration Search (DIS), which optimizes inference paths through block-wise searching with permutation and layer selection from different source models.

search process, we implement multi-fidelity optimization that reduces search costs while efficiently finding both task-specific optimal solutions and Pareto-optimal configurations across multiple reasoning dimensions.

3.2. Search Space

3.2.1. LAYER-WISE FUSION SEARCH SPACE

Layer-wise merging combines corresponding layers from multiple models to create a new model. While effective, current approaches typically apply uniform merging methods and hyperparameters across all layers, using the entire set of candidate models, which might be too coarse-grained and potentially problematic. To illustrate this concern, we conduct an analysis using TIES merge (Yadav et al., 2024), one of the most robust merging methods, on the GSM8K benchmark. As shown in Figure 3 (a), when applying TIES merge with same hyperparameters across different model combinations, the accuracy varies dramatically from 1% to 64.5%. Furthermore, Figure 3 (b) demonstrates that even with a fixed model combination (Math+Code), different hyperparameter settings lead to substantial performance variations, ranging from 34.9% to 64.5%. These results reveal two critical challenges in layer-wise merging: the selection of candidate models and the determination of hyperparameters. Both factors significantly impact the final performance, even for well-established methods like TIES. Manual tuning of these choices is not only labor-intensive but also makes it challenging to find optimal configurations.

To address these limitations and motivated by how different layers in neural networks serve distinct purposes, from basic feature extraction to complex task-specific processing, we design a fine-grained layer-wise merging search space (LFS).

Our search space is illustrated in Figure 2 (a), we partition the model’s L layers into G consecutive groups, where layers within each group share the same merging coefficients. These coefficients determine: (1) the selection of source models from the candidate pool, (2) the choice of merging algorithms, and (3) the corresponding hyperparameters for the chosen merging method. Furthermore, we introduce a component-wise decomposition strategy. Specifically, we partition the parameters within each Transformer layer into C component groups. When $C = 1$, the entire layer is treated as a single unit. When $C = 3$, we decompose the layer into three groups: MLP-related parameters, attention mechanism parameters, and layer normalization parameters. This decomposition allows for the application of component-specific hyperparameters during the merging process.

We define the merging coefficients $x \in \mathbb{R}^{G \times C \times (1+H)}$, where G represents the number of layer groups, C denotes the number of components per layer, and $1 + H$ dimensions specify the merging method selection and hyperparameters of all candidate merging methods. We use four well-established merging methods: Task Arithmetic, TIES-Merging, SLERP, and Linear Merging. See Section A.2 for more descriptions of the methods. LFS provides a fine-grained and flexible search space for model merging, which not only enables precise optimization of the fusion but also maximizes the potential of layer-wise merging.

3.2.2. DEPTH-WISE INTEGRATION SEARCH SPACE

Large Language Models (LLMs) exhibit hierarchical language understanding, with knowledge transformation progressing sequentially from word-level comprehension to abstract conceptual understanding. Recent research has increasingly focused on the behavior of transformer layers.

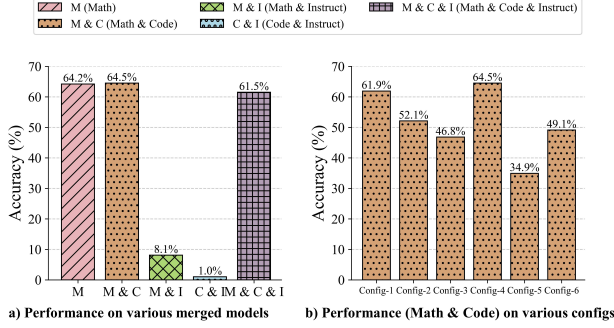


Figure 3. Performance of TIES merges on GSM8K: (a) comparison of different source model combinations and (b) various configurations with Math and Code as source models. We set the scaling term and parameter retention ratio in reasonable ranges of $[0.5, 1.0]$ and $[0.5, 0.7, 0.9]$, respectively. See Table 7 for detailed configuration information.

Meng et al. (2022) and Geva et al. (2022) explored the distribution of knowledge across different layers. Lad et al. examined the robustness of transformer-based large language models by analyzing the effects of layer deletion and swapping. Sun et al. (2024) show that lower and final layers differ from middle layers, which demonstrate uniformity and robustness to reordering and parallelization for certain tasks. This hierarchical relationship between layers remain unexplored in the context of model merging. To fill this gap, we introduce the Depth-wise Integration Search Space (DIS), which preserves the original weights of individual layers while optimizing the inference pathway.

As depicted in Figure 2 (b), DIS is characterized by three parameters: depth granularity D , number of candidate models M , and repeat factor R . These parameters partition transformer layers into $B = L/D$ consecutive blocks, where each block encompasses $D \times M \times R$ candidate layers. The search space is characterized by merging coefficients $x = \{(\mathbf{s}^{(i)}, \mathbf{p}^{(i)})\}_{i=1}^B$, where selection vector $\mathbf{s}^{(i)} \in \{0, 1\}^{M \times D \times R}$ determines layer activation and permutation vector $\mathbf{p}^{(i)} \in \{0, 1, \dots, P-1\}$ with $P = (D \times M \times R)! / (R!)^{M \times D}$ specifies layer ordering. When no layers are selected in a block ($\mathbf{s}^{(i)} = 0$), we implement a layer retention strategy that preserves model depth by defaulting to base model layers. To maintain architectural coherence, we introduce scaling factors $\{o_1, \dots, o_B\}$ to normalize the output of each block (Akiba et al., 2024).

This parametrization enables a rich set of architectural operations, including layer pruning, stacking, repetition, and reordering, with the scope of these operations controlled by the granularity parameter D . At $D = 1$, the search space emphasizes layer-wise interactions at corresponding positions across candidate models. As D increases, the framework accommodates more complex integration patterns and cross-depth layer interactions. We hypothesize that LFS and DIS

might serve complementary roles. Our intuition is that LFS, with its fine-grained feature fusion, could be better suited for combining models with similar concepts, while DIS’s preservation of processing blocks might be more effective when merging models from complementary domains.

3.3. Multi-Fidelity Optimization

Although optimization of model merging requires less computation compared to searching for optimal hyperparameters for neural network structures and the model training process (Yu & Zhu, 2020; Elsken et al., 2019), evaluating large language models on extensive validation datasets remains computationally intensive. We optimize the process using cost-efficient Multi-Fidelity Optimization (MFO) (Peherstorfer et al., 2018), leveraging evaluations across different fidelity levels from fast but less accurate low-fidelity to slow but more accurate high-fidelity.

The optimization objective can be formulated as:

$$x^* \in \arg \min_{x \in \Lambda} c(x, b) = \arg \min_{x \in \Lambda} \mathcal{L}(\mathcal{D}_{\text{val}}; x, b) \quad (1)$$

Here, we use evaluation samples as fidelity types. Each configuration is evaluated with varying budgets $b_{\min} \leq b \leq b_{\max}$, where the budget determines the validation dataset size. Using smaller budgets provides a cheaper proxy of the true cost function (measured at b_{\max}).

Our implementation extends SMAC (Lindauer et al., 2022) by establishing a hierarchical evaluation framework parameterized by b_{\max} , b_{\min} , and spacing factor η . Using Successive Halving (Jamieson & Talwalkar, 2016), each bracket i starts with n_i configurations at budget b_i , iteratively halving configurations and increasing budgets by η until reaching b_{\max} . Higher brackets begin with fewer configurations but larger budgets. A Random Forest surrogate model (Breiman, 2001) guides configuration selection through Expected Improvement, balancing exploration at low fidelities with exploitation at high fidelities. See Section A.3 for more descriptions of the optimization.

3.3.1. SINGLE OBJECTIVE OPTIMIZATION

We use single-objective optimization to maximize task-specific performance. The cost function for each task is defined as:

$$c_i(x) = \arg \min_{x \in \Lambda} \mathcal{L}(\mathcal{D}_i; x, b_{\min}, b_{\max}) \quad (2)$$

where $c_i(x)$ represents an optimization objective over the parameter space x for a specific task dataset \mathcal{D}_i . The loss function \mathcal{L} measures the model’s performance on the target task dataset.

We define different optimization objectives using task-specific datasets: GSMPlus (Li et al., 2024) for mathematical reasoning, MBPP (Austin et al., 2021) validation set for programming capabilities, and MMLU (Hendrycks et al., 2020) validation set for general reasoning.

3.3.2. MULTI OBJECTIVE OPTIMIZATION

To develop comprehensive reasoning models, we employ ParEGO (Knowles, 2006) for multi-objective optimization to identify Pareto-optimal solutions across different objectives. The algorithm converts different cost values into a single cost using a parameterized scalarizing weight vector. By varying this weight vector at each iteration, ParEGO gradually builds an approximation of the entire Pareto front. Initially, the algorithm normalizes the k cost functions to the $[0, 1]$ interval.

In each step, the algorithm randomly selects a weight vector λ from a set of uniformly distributed vectors, defined as:

$$\Lambda = \left\{ \lambda = (\lambda_1, \lambda_2, \dots, \lambda_k) \mid \sum_{j=1}^k \lambda_j = 1 \wedge \forall j, \lambda_j = \frac{l}{s}, l \in \{0, \dots, s\} \right\}$$

The size of this set is determined by $|\Lambda| = \binom{s+2}{2}$, where s controls the total number of possible vectors. The scalar cost for each solution is calculated using the augmented Tchebycheff function, where ρ represents a small positive constant:

$$c_{\text{agg}}(x; \lambda) = \max_{j=1}^k (\lambda_j \cdot c_j(x)) + \rho \sum_{j=1}^k \lambda_j \cdot c_j(x) \quad (3)$$

4. Experiments

4.1. Experimental Setting

Source Models We use LLaMA-family models (Touvron et al., 2023) as our base model set, including WizardLM-13B (Xu et al., 2023), WizardMath-13B (Luo et al., 2023a), and llama-2-13b-code-alpaca (Chaudhary, 2023). All these models are fine-tuned from Llama-2-13b, ensuring a shared loss landscape. We exclude WizardCoder-Python-13B (Luo et al., 2023b) as it uses CodeLlama-13b-Python (Roziere et al., 2023) as its pre-trained backbone, resulting in a different loss landscape.

Datasets We select separate datasets for search and evaluation. For searching, we use GSMPlus (Li et al., 2024) for mathematical reasoning, MBPP (Austin et al., 2021) samples for code understanding, and MMLU (Hendrycks et al., 2020) validation samples for general knowledge. For evaluation, we employ established benchmark test sets: GSM8K

and MATH for mathematical reasoning, MBPP and HumanEval (Chen et al., 2021) for code generation, and the MMLU test set for general knowledge assessment. See Section A.4 and A.5 for more details.

Search Spaces As described in the method section, within LFS we implement four merging methods: Task Arithmetic, TIES-Merging, Linear-merging, and Slerp. We set the number of layer groups to $G = 4$ and the number of component groups per layer to $C = 3$. For DIS, we evaluate two configurations: Configuration 1 with depth granularity $D = 1$, number of candidate models $M = 3$, and repeat factor $R = 1$; Configuration 2 with $D = 1$, $M = 1$, and $R = 2$. Both configurations keep $D = 1$ to manage optimization complexity. We focus on studying layer-wise interactions between corresponding positions across candidate models. See A.6 for more details.

Optimization Our implementation builds upon SMAC (Lindauer et al., 2022), with domain-specific budget allocations for optimization tasks. Mathematical reasoning tasks receive 100-1000 samples to explore complex solution spaces, code reasoning uses 300 samples (200 training, 100 validation), and we sample 50% of MMLU validation data within 100-700 sample bounds. These budget ranges remain consistent when conducting multi-objective optimization across multiple datasets within these domains. We configured the search trials based on the complexity of each search space. We allocated 500 search trials for LFS and 1000 for the broader DIS search space, using initial candidate models as starting points to improve optimization efficiency.

4.2. Results

4.2.1. SINGLE OBJECTIVE OPTIMIZATION

Layer-wise Fusion Using three source models (Math, Code, and LM) optimized for mathematical, coding, and general reasoning tasks respectively, we developed three specialized models through LFS: MATH-LFS, CODE-LFS, and GEN-LFS. Table 1 presents the performance of these models across five benchmarks. Our results demonstrate that MATH-LFS achieves a 4.24% improvement over the best performance of source models on GSM8k, CODE-LFS shows modest gains on MBPP, and GEN-LFS exhibits a 1.88% improvement on MMLU. These MATH-LFS gains are especially surprising, given that the base model was already finetuned for improve GSM8k performance - it appears that its arithmetic performance could be further improved through merging with the coding and instruction tuning model.

Beyond these task-specific enhancements, we observe that LFS-searched models also demonstrate improved performance in other reasoning capabilities, with MATH-LFS showing particular strength in both common reasoning and

Table 1. Performance comparison of merged models combining WizardLM-13B (LM), WizardMath-13B (Math), and llama-2-13b-codealpaca (Code). For single-objective optimization, improvements over source models are shown in blue. For multi-objective optimization, improvements over the best base model (MATH) are shown in blue in the Average column.

Method	Model	Source*	Search*	Common		Math		Code		Average
				MMLU	GSM8K	MATH	MBPP	HumanEval		
Base	MATH	–	–	52.04	64.22	13.70	18.20	7.32	31.10	
	CODE	–	–	52.79	0.00	0.00	27.20	23.17	20.63	
	LM	–	–	53.43	3.79	0.00	33.40	38.41	25.81	
Basic	Ties	M+C+L	–	54.67	61.56	10.58	27.40	23.17	35.48 (+4.38)	
	Task Arith	M+C+L	–	54.85	57.99	12.06	26.22	24.04	35.03 (+3.93)	
	Linear	M+C+L	–	55.13	57.09	9.98	29.80	18.90	34.18 (+3.08)	
Single-Obj	MATH-LFS	M+C+L	1	54.52	68.46 (+4.24)	10.42	28.20	17.07	–	
	CODE-LFS	M+C+L	2	53.36	49.73	9.30	33.60 (+0.20)	14.63	–	
	GEN-LFS	M+C+L	3	55.31 (+1.88)	33.81	3.82	30.80	16.46	–	
	GEN-DIS-0	M+C+L	3	54.72 (+1.29)	16.98	1.14	12.40	9.76	–	
	GEN-DIS-1	L	3	54.76 (+1.33)	1.74	0.06	16.80	18.29	–	
Multi-Obj	MULTI-LFS-0	M+C+L	1-3	55.03	63.08	11.76	32.60	21.95	36.88 (+5.78)	
	MULTI-LFS-1	M+C+L	1-3	54.70	66.94	11.38	30.60	23.78	37.48 (+6.38)	
	MULTI-LFS-2	M+C+L	1-3	54.67	65.13	11.06	30.40	20.73	36.40 (+5.30)	
	MULTI-LFS-3	M+C+L	1-3	54.99	65.50	9.42	30.20	23.17	36.66 (+5.56)	
	MULTI-LFS-4	M+C+L	1-3	54.77	66.79	12.06	31.80	24.40	37.96 (+6.86)	

*Dataset Index: 1=GSMPlus, 2=MBPP_{val}, 3=MMLU_{val}

*M+C+L = Math+Code+LM

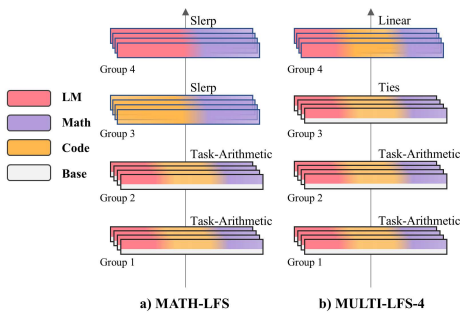


Figure 4. Visualization of LFS-searched models

code generation tasks. In comparison with alternative merging methods including TIES, Task Arithmetic, and linear merging (with hyperparameter search ranges detailed in Table 8), our LFS method achieves superior performance on the targeted optimization objectives, demonstrating the effectiveness of our approach in single task optimization. The architecture of MATH-LFS, as illustrated in Figure 4 (a), divides the model layers into four groups (G=4), where Task Arithmetic merge is employed for groups 1 and 2, while the subsequent layer groups 3 and 4 utilize SLERP merge with different model combinations - Math-Code and Math-LM respectively. The full architecture parameters can be found in Table 11. Notably, we found that HumanEval (Chen et al., 2021) is very sensitive to parameter changes. When merging the LM with other models, performance dropped for all methods. This may be due to the nature of the task and the small test set of only 164 samples.

Depth-wise Integration We evaluated two DIS search configurations: Configuration 1 using three candidate models (Code, Math, and LM) with depth granularity 1 and repeat factor 1; and Configuration 2 using a single candidate model (the corresponding source model for specific objective) with depth granularity 1 and repeat factor 2. Using these configurations, we similarly optimized for mathematical, coding, and general reasoning tasks respectively. DIS demonstrated effectiveness only in general reasoning tasks, yielding GEN-DIS-0 and GEN-DIS-1. Our results, as presented in Table 1, demonstrate that both models achieved improvements, exceeding 1% over the source models on the MMLU benchmark. GEN-DIS-0 exhibited enhanced performance not only on the optimization objective but also demonstrated benefits on auxiliary tasks, showing improvement on the GSM8K. A detailed breakdown of performance across MMLU categories is presented in Table 9.

We visualize the network in Figure 5. The complete set of architectural parameters can be found in Table 12. GEN-DIS-0 exhibited a predominantly stable selection of LM layers in early layers, gradually incorporating other source model layers with stacking behavior in middle and later layers. Similarly, GEN-DIS-1 demonstrated no layer repetition in early layers but showed emergence of layer repetition patterns after layer 15. Notably, although improvements were observed in common reasoning task, we found no superior configurations for mathematical and code reasoning tasks, suggesting varying sensitivity to layer ordering across different tasks. To further explore our methodology, we

Table 2. Performance of models merged via LFS and DIS on other Reasoning Tasks. LFS+DIS represents using LFS-merged model as an additional source model for DIS search. Numbers in blue indicate improvements over the best source model.

Benchmark	Source Models				Merging Results		
	Math	Code	LM	LM_JA	LFS	DIS	LFS+DIS
LogiQA	29.65	25.81	28.57	–	30.88 (+1.23)	29.34 (-0.31)	31.64 (+1.99)
OpenBookQA	34.20	34.80	34.40	–	37.60 (+2.80)	37.40 (+2.60)	38.60 (+3.80)
OpenBookQA+f	39.20	44.20	46.20	–	47.00 (+0.80)	47.40 (+1.20)	47.80 (+1.60)
PIQA	79.77	79.92	79.95	–	80.93 (+0.98)	79.02 (-0.93)	80.03 (+0.08)
SocialIQA	46.82	46.77	51.09	–	51.14 (+0.05)	50.50 (-0.59)	50.17 (-0.92)
MGSM_JA	8.00	4.00	10.40	–	17.60 (+7.20)	15.20 (+4.80)	22.00 (+10.60)
MGSM_JA	8.00	–	–	8.80	16.40 (+7.60)	21.60 (+12.80)	19.60 (+10.80)

*LM_JA denotes ELYZA-japanese-Llama-2-13b

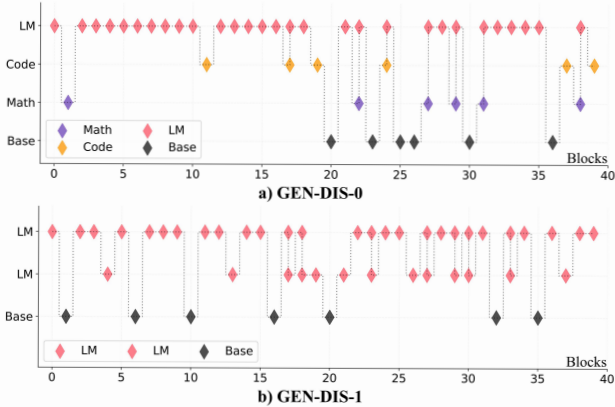


Figure 5. Visualization of DIS model architecture. The x-axis represents block indices from 1 to 40, and the y-axis indicates the selected layer in each block.

extend our investigation to additional tasks.

Expanding to other tasks We further evaluated our method on diverse reasoning tasks including LogicQA (Liu et al., 2020), OpenBookQA (Mihaylov et al., 2018), PIQA (Bisk et al., 2020), SocialIQA (Sap et al., 2019), and MGSM Japanese (Sap et al., 2019), using validation datasets for searching and test sets for evaluation. For OpenBookQA, we tested with and without relevant facts in the prompt. We incorporated ELYZA-japanese-Llama-2-13b (Sasaki et al., 2023) alongside our base models (LM, Math, Code) for MGSM Japanese tasks. See Section A.8 for implementation details. Results are presented in Table 2. For most tasks, LFS+DFS shows promising results with significant improvements across benchmarks, notably 3.80% on OpenBookQA and up to 10.8 points on MGSM_JA. In addition to LFS that consistently delivers positive improvements, DFS shows occasional degradation in LogiQA and PIQA. The results particularly highlight the effectiveness of our method in cross-lingual reasoning tasks, DIS demonstrates notable effectiveness with improvements up to 12.80 points, supporting our hypothesis that DIS excels when handling models trained on complementary domains. The architec-

tural parameters can be found in Tables 13 and 14.

4.2.2. MULTI OBJECTIVE OPTIMIZATION

Given the task-specific nature of DIS search and the more robust merging capabilities of LFS, we conducted our multi objective search on LFS with three optimization objectives: mathematical reasoning, code generation, and general reasoning. Our optimization yielded five Pareto-optimal solutions, denoted as MULTI-LFS-0 to MULTI-LFS-4, with their performance metrics presented in Table 1. These solutions achieved significant improvements, ranging from 5.30 to 6.86 points on average compared to the best base model. When comparing our results with existing merging approaches such as Ties, task arithmetic, and linear merging, our method achieves better trade-offs along the Pareto frontier while maintaining higher average performance across all benchmarks. This demonstrates the effectiveness of our multi-objective optimization strategy in finding superior model configurations that balance diverse task requirements.

As visualized in Figure 4 (b), our analysis of MULTI-LFS-4 reveals an interesting layer-wise merging pattern: Task Arithmetic is optimal for groups 1 and 2, while groups 3 and 4 employ Ties and linear merging strategies. Unlike the single-objective search-derived MATH-LFS, MULTI-LFS-4 shows a preference for incorporating layers from all source models during the merging process, resulting in better preservation of comprehensive information.

Table 3. Distribution of searching trials across different budget levels for MATH-LFS and GEN-DIS-1.

	MATH-LFS			GEN-DIS-1			
	100	300	1000	0	100	300	700
Trail Count	263	152	85	196	311	307	186
Percentage (%)	52.6	30.4	17.0	19.6	31.1	30.7	18.6

4.2.3. EFFICIENCY ANALYSIS

Our Multi-Fidelity Optimization (MFO) framework dynamically adjusts the budget allocation during the search process,

Table 4. Ablation study on granularity (G) and component groups (C) for MATH-LFS search.

Component Groups	Layer Groups (G)			
	10	4	2	1
$C=3$	66.79	68.46	67.82	66.41
$C=1$	66.41	68.08	67.24	66.41

Table 5. Ablation study on layer retention for GEN-DIS-1 model. GEN-DIS-1-NR denotes GEN-DIS-1 without layer retention.

Model	MMLU	GSM8K	MATH	MBPP	HumanEval
LM	53.43	3.79	0.00	33.40	38.41
GEN-DIS-1	54.76 ↑	1.74	0.06	16.80	18.29
GEN-DIS-NR	53.68 ↑	1.82	0.02	9.80	4.88

where the budget is defined as the validation dataset size used for searching. We implemented different search iterations and budget ranges based on the search space size and specific tasks. Here, we analyze the budget distribution during the search process using MATH-LFS and GEN-DIS-1 as examples (see Table 10 for complete budget details). As shown in Table 3, for MATH-LFS, we conducted 500 search trials with a budget range of (100, 1000), divided into three levels: 100, 300, and 1000. Our analysis reveals that only 17% of the search trials utilized the full budget, while over 52% of the evaluations were conducted with the minimum budget of 100. For GEN-DIS-1, considering that DIS search typically explores deeper architectures, we imposed a maximum layer constraint of 50 to manage computational costs. Configurations exceeding this depth constraint were assigned a reward of 0 without evaluation, resulting in zero budget allocation. Consequently, out of the initial 1000 trials in DIS, 804 were effective search trials, with only 18.6% utilizing the full evaluation budget, showing that our multi-fidelity approach significantly reduced computational resource consumption during the search process while consistently discovering high-quality solutions.

5. Ablations and Analysis

5.1. Impact of granularity in LFS

To examine the effect of granularity in layer-wise fusion search space, we conducted ablation studies to examine the effect of granularity in LFS by varying the number of layer groups (G) and component groups (C). Table 4 shows that increasing G from 1 to 4 consistently improves GSM8K accuracy, demonstrating the benefits of more fine-grained layer control. However, performance decreases when G reaches 10, likely due to the growth in search space exceeding our search algorithm’s capability within the given trials. Our analysis also shows that increasing C from 1 to 3 improves performance, though these gains are smaller compared to those from layer-wise refinement.

Table 6. Performance comparison of source models and SFS-search results

Benchmark	Source Models			SFS Results		
	Math	Code	LM	SFS-0	SFS-1	SFS-2
MMLU	52.04	52.79	53.43	52.03	51.91	53.63 ↑
GSM8K	64.22	0.00	3.79	63.91 ↓	0.00	6.52
MATH	13.70	0.00	0.00	13.58	0.00	0.08
MBPP	18.20	27.20	33.40	18.20	28.60 ↑	30.40
HumanEval	7.32	23.17	38.41	7.32	24.39	34.15

5.2. Impact of layer retention in DIS

To explore the layer retention strategy in our DIS search space, we conducted a comparative experiment. Specifically, we modified the DIS-GEN-1 configuration by replacing the layer retention strategy with direct layer deletion, resulting in the DIS-GEN-RN. As shown in Table 5, although DIS-GEN-RN marginally outperformed the baseline language model on MMLU tasks, its performance still fell short compared to our proposed layer retention approach. This result shows that directly deleting layers degrades model performance while retaining layers is more effective.

5.3. Search only on scales

Several findings show that fine-tuning (Zhang et al., 2024) or scaling (Christ et al., 2024) task-specific neurons can improve model performance. To evaluate these claims and to verify that our DIS search space (which includes scales) is not simply re-scaling layers, we further evaluate Scale-Factor Search Space (SFS) that optimizes tasks by searching scaling factors to weights and layer outputs. As before, we apply our framework and obtain three SFS models: SFS-MATH, SFS-CODE, and SFS-GEN, each initialized from specialized base models. As shown in Table 6, Results show a decline in mathematical performance and slight improvements in code and reasoning tasks, though gains are modest compared to LFS and DIS, showing that scale optimization alone is not sufficient to explain the DIS effectiveness.

6. Conclusions and Future Work

In this work, we presented a Multi-Fidelity Framework for Automated Model Merging that introduces two complementary search spaces: Layer-wise Fusion Search Space (LFS) and Depth-wise Integration Search Space (DIS). LFS enables fine-grained layer-wise merging, and DIS optimizes sequential layer arrangements while preserving individual layer weights. We show automated model merging not only works, but is quite effective, demonstrating strong performance in both single-objective and multi-objective scenarios, achieving a 4.24% improvement on the GSM8K challenge task with only 17% of the full budget within 500 trials, and a 6.86% improvement in multi-objective perfor-

mance using 18.6% of the full budget within 1000 trials. When extended to various benchmarks, our method consistently shows promising results without any additional tuning. Overall, our work provides an efficient and flexible framework for automated model merging that achieves effective improvements with reduced computational costs.

References

- Akiba, T., Shing, M., Tang, Y., Sun, Q., and Ha, D. Evolutionary optimization of model merging recipes. *arXiv preprint arXiv:2403.13187*, 2024.
- Austin, J., Odena, A., Nye, M., Bosma, M., Michalewski, H., Dohan, D., Jiang, E., Cai, C., Terry, M., Le, Q., et al. Program synthesis with large language models. *arXiv preprint arXiv:2108.07732*, 2021.
- Bi, X., Chen, D., Chen, G., Chen, S., Dai, D., Deng, C., Ding, H., Dong, K., Du, Q., Fu, Z., et al. Deepseek llm: Scaling open-source language models with longtermism. *arXiv preprint arXiv:2401.02954*, 2024.
- Bisk, Y., Zellers, R., Gao, J., Choi, Y., et al. Piqa: Reasoning about physical commonsense in natural language. In *Proceedings of the AAAI conference on artificial intelligence*, volume 34, pp. 7432–7439, 2020.
- Breiman, L. Random forests. *Machine learning*, 45:5–32, 2001.
- Chaudhary, S. Code alpaca: An instruction-following llama model for code generation. *GitHub repository*, 2023.
- Chen, M., Tworek, J., Jun, H., Yuan, Q., de Oliveira Pinto, H. P., Kaplan, J., Edwards, H., Burda, Y., Joseph, N., Brockman, G., Ray, A., Puri, R., Krueger, G., Petrov, M., Khlaaf, H., Sastry, G., Mishkin, P., Chan, B., Gray, S., Ryder, N., Pavlov, M., Power, A., Kaiser, L., Bavarian, M., Winter, C., Tillet, P., Such, F. P., Cummings, D., Plappert, M., Chantzis, F., Barnes, E., Herbert-Voss, A., Guss, W. H., Nichol, A., Paino, A., Tezak, N., Tang, J., Babuschkin, I., Balaji, S., Jain, S., Saunders, W., Hesse, C., Carr, A. N., Leike, J., Achiam, J., Misra, V., Morikawa, E., Radford, A., Knight, M., Brundage, M., Murati, M., Mayer, K., Welinder, P., McGrew, B., Amodei, D., McCandlish, S., Sutskever, I., and Zaremba, W. Evaluating large language models trained on code. 2021.
- Christ, B. R., Gottesman, Z., Kropko, J., and Hartvigsen, T. Math neurosurgery: Isolating language models’ math reasoning abilities using only forward passes. *arXiv preprint arXiv:2410.16930*, 2024.
- Cobbe, K., Kosaraju, V., Bavarian, M., Chen, M., Jun, H., Kaiser, L., Plappert, M., Tworek, J., Hilton, J., Nakano, R., et al. Training verifiers to solve math word problems. *arXiv preprint arXiv:2110.14168*, 2021.
- Elsken, T., Metzen, J. H., and Hutter, F. Neural architecture search: A survey. *Journal of Machine Learning Research*, 20(55):1–21, 2019.
- Gao, L., Tow, J., Abbasi, B., Biderman, S., Black, S., DiPofi, A., Foster, C., Golding, L., Hsu, J., Le Noac’h, A., Li, H., McDonell, K., Muennighoff, N., Ociepa, C., Phang, J., Reynolds, L., Schoelkopf, H., Skowron, A., Sutawika, L., Tang, E., Thite, A., Wang, B., Wang, K., and Zou, A. A framework for few-shot language model evaluation, 07 2024. URL <https://zenodo.org/records/12608602>.
- Geva, M., Caciularu, A., Wang, K. R., and Goldberg, Y. Transformer feed-forward layers build predictions by promoting concepts in the vocabulary space. *arXiv preprint arXiv:2203.14680*, 2022.
- Guo, D., Zhu, Q., Yang, D., Xie, Z., Dong, K., Zhang, W., Chen, G., Bi, X., Wu, Y., Li, Y., et al. Deepseek-coder: When the large language model meets programming—the rise of code intelligence. *arXiv preprint arXiv:2401.14196*, 2024.
- Hendrycks, D., Burns, C., Basart, S., Zou, A., Mazeika, M., Song, D., and Steinhardt, J. Measuring massive multitask language understanding. *arXiv preprint arXiv:2009.03300*, 2020.
- Hendrycks, D., Burns, C., Kadavath, S., Arora, A., Basart, S., Tang, E., Song, D., and Steinhardt, J. Measuring mathematical problem solving with the math dataset. *NeurIPS*, 2021.
- Hutter, F., Hoos, H. H., and Leyton-Brown, K. Sequential model-based optimization for general algorithm configuration. In *Learning and Intelligent Optimization: 5th International Conference, LION 5, Rome, Italy, January 17-21, 2011. Selected Papers 5*, pp. 507–523. Springer, 2011.
- Ilharco, G., Ribeiro, M. T., Wortsman, M., Gururangan, S., Schmidt, L., Hajishirzi, H., and Farhadi, A. Editing models with task arithmetic. *arXiv preprint arXiv:2212.04089*, 2022.
- Jamieson, K. and Talwalkar, A. Non-stochastic best arm identification and hyperparameter optimization. In *Artificial intelligence and statistics*, pp. 240–248. PMLR, 2016.
- Jiang, A. Q., Sablayrolles, A., Mensch, A., Bamford, C., Chaplot, D. S., Casas, D. d. l., Bressand, F., Lengyel, G., Lample, G., Saulnier, L., et al. Mistral 7b. *arXiv preprint arXiv:2310.06825*, 2023.

- Knowles, J. Parego: A hybrid algorithm with on-line landscape approximation for expensive multiobjective optimization problems. *IEEE transactions on evolutionary computation*, 10(1):50–66, 2006.
- Kwon, W., Li, Z., Zhuang, S., Sheng, Y., Zheng, L., Yu, C. H., Gonzalez, J. E., Zhang, H., and Stoica, I. Efficient memory management for large language model serving with pagedattention. In *Proceedings of the ACM SIGOPS 29th Symposium on Operating Systems Principles*, 2023.
- Lad, V., Gurnee, W., and Tegmark, M. The remarkable robustness of llms: Stages of inference?, 2024. URL <https://arxiv.org/abs/2406.19384>.
- Li, L., Jamieson, K., DeSalvo, G., Rostamizadeh, A., and Talwalkar, A. Hyperband: A novel bandit-based approach to hyperparameter optimization. *Journal of Machine Learning Research*, 18(185):1–52, 2018.
- Li, Q., Cui, L., Zhao, X., Kong, L., and Bi, W. Gsm-plus: A comprehensive benchmark for evaluating the robustness of llms as mathematical problem solvers. *arXiv preprint arXiv:2402.19255*, 2024.
- Lindauer, M., Eggenberger, K., Feurer, M., Biedenkapp, A., Deng, D., Benjamins, C., Ruhkopf, T., Sass, R., and Hutter, F. Smac3: A versatile bayesian optimization package for hyperparameter optimization. *Journal of Machine Learning Research*, 23(54):1–9, 2022. URL <http://jmlr.org/papers/v23/21-0888.html>.
- Liu, J., Cui, L., Liu, H., Huang, D., Wang, Y., and Zhang, Y. Logiqa: A challenge dataset for machine reading comprehension with logical reasoning. *arXiv preprint arXiv:2007.08124*, 2020.
- Luo, H., Sun, Q., Xu, C., Zhao, P., Lou, J., Tao, C., Geng, X., Lin, Q., Chen, S., and Zhang, D. Wizardmath: Empowering mathematical reasoning for large language models via reinforced evol-instruct. *arXiv preprint arXiv:2308.09583*, 2023a.
- Luo, Z., Xu, C., Zhao, P., Sun, Q., Geng, X., Hu, W., Tao, C., Ma, J., Lin, Q., and Jiang, D. Wizardcoder: Empowering code large language models with evol-instruct. *arXiv preprint arXiv:2306.08568*, 2023b.
- Mendoza, H., Klein, A., Feurer, M., Springenberg, J. T., and Hutter, F. Towards automatically-tuned neural networks. In *Workshop on automatic machine learning*, pp. 58–65. PMLR, 2016.
- Meng, K., Bau, D., Andonian, A., and Belinkov, Y. Locating and editing factual associations in gpt. *Advances in Neural Information Processing Systems*, 35:17359–17372, 2022.
- Mihaylov, T., Clark, P., Khot, T., and Sabharwal, A. Can a suit of armor conduct electricity? a new dataset for open book question answering. *arXiv preprint arXiv:1809.02789*, 2018.
- OpenAI, Achiam, J., Adler, S., Agarwal, S., Ahmad, L., Akkaya, I., Aleman, F. L., Almeida, D., Altenschmidt, J., Altman, S., Anadkat, S., et al. Gpt-4 technical report. *arXiv preprint arXiv:2303.08774*, 2023.
- Peherstorfer, B., Willcox, K., and Gunzburger, M. Survey of multifidelity methods in uncertainty propagation, inference, and optimization. *Siam Review*, 60(3):550–591, 2018.
- Perrone, V., Jenatton, R., Seeger, M., and Archambeau, C. Multiple adaptive bayesian linear regression for scalable bayesian optimization with warm start. *arXiv preprint arXiv:1712.02902*, 2017.
- Ramesh, A., Pavlov, M., Goh, G., Gray, S., Voss, C., Radford, A., Chen, M., and Sutskever, I. Zero-shot text-to-image generation. In *International conference on machine learning*, pp. 8821–8831. Pmlr, 2021.
- Roziere, B., Gehring, J., Gloeckle, F., Sootla, S., Gat, I., Tan, X. E., Adi, Y., Liu, J., Sauvestre, R., Remez, T., et al. Code llama: Open foundation models for code. *arXiv preprint arXiv:2308.12950*, 2023.
- Saharia, C., Chan, W., Saxena, S., Li, L., Whang, J., Denton, E. L., Ghasemipour, K., Gontijo Lopes, R., Karagol Ayan, B., Salimans, T., et al. Photorealistic text-to-image diffusion models with deep language understanding. *Advances in neural information processing systems*, 35:36479–36494, 2022.
- Sap, M., Rashkin, H., Chen, D., LeBras, R., and Choi, Y. Socialiqa: Commonsense reasoning about social interactions. *arXiv preprint arXiv:1904.09728*, 2019.
- Sasaki, A., Hirakawa, M., Horie, S., Nakamura, T., Pasaglia, S., and Oba, D. Elyza-japanese-llama-2-13b, 2023. URL <https://huggingface.co/elyza/ELYZA-japanese-Llama-2-13b>.
- Snoek, J., Larochelle, H., and Adams, R. P. Practical bayesian optimization of machine learning algorithms. *Advances in neural information processing systems*, 25, 2012.
- Snoek, J., Rippel, O., Swersky, K., Kiros, R., Satish, N., Sundaram, N., Patwary, M., Prabhat, M., and Adams, R. Scalable bayesian optimization using deep neural networks. In *International conference on machine learning*, pp. 2171–2180. PMLR, 2015.

-
- Springenberg, J. T., Klein, A., Falkner, S., and Hutter, F. Bayesian optimization with robust bayesian neural networks. *Advances in neural information processing systems*, 29, 2016.
- Sun, Q., Pickett, M., Nain, A. K., and Jones, L. Transformer layers as painters. *arXiv preprint arXiv:2407.09298*, 2024.
- Touvron, H., Lavril, T., Izacard, G., Martinet, X., Lachaux, M.-A., Lacroix, T., Rozière, B., Goyal, N., Hambro, E., Azhar, F., et al. Llama: Open and efficient foundation language models. *arXiv preprint arXiv:2302.13971*, 2023.
- Utans, J. Weight averaging for neural networks and local resampling schemes. In *Proc. AAAI-96 Workshop on Integrating Multiple Learned Models*. AAAI Press, pp. 133–138. Citeseer, 1996.
- White, T. Sampling generative networks. *arXiv preprint arXiv:1609.04468*, 2016.
- Xu, C., Sun, Q., Zheng, K., Geng, X., Zhao, P., Feng, J., Tao, C., and Jiang, D. Wizardlm: Empowering large language models to follow complex instructions. *arXiv preprint arXiv:2304.12244*, 2023.
- Yadav, P., Tam, D., Choshen, L., Raffel, C. A., and Bansal, M. Ties-merging: Resolving interference when merging models. *Advances in Neural Information Processing Systems*, 36, 2024.
- Yu, L., Yu, B., Yu, H., Huang, F., and Li, Y. Language models are super mario: Absorbing abilities from homologous models as a free lunch. In *Forty-first International Conference on Machine Learning*, 2024.
- Yu, T. and Zhu, H. Hyper-parameter optimization: A review of algorithms and applications. *arXiv preprint arXiv:2003.05689*, 2020.
- Zhang, W., Wan, C., Zhang, Y., Cheung, Y.-m., Tian, X., Shen, X., and Ye, J. Interpreting and improving large language models in arithmetic calculation. *arXiv preprint arXiv:2409.01659*, 2024.
- Zhu, Q., Guo, D., Shao, Z., Yang, D., Wang, P., Xu, R., Wu, Y., Li, Y., Gao, H., Ma, S., et al. Deepseek-coder-v2: Breaking the barrier of closed-source models in code intelligence. *arXiv preprint arXiv:2406.11931*, 2024.

A. Detailed Experimental Settings

A.1. Details of TIES Configuration for Math and Code Model Merging on GSM8K

Table 7. Performance Comparison with Different Parameters of Ties Merging Method

Parameters	Configuration					
Ratio to retain parameters	0.7	0.5	0.7	0.5	0.9	0.9
Scaling Coefficient	1.0	0.5	0.5	1.0	0.5	1.0
Performance on GSM8k	61.94	52.08	46.78	64.52	34.87	49.05

A.2. Descriptions of Existing Model Merging Methods in Layer-wise Fusion Search Space (LFS)

Task Arithmetic enhance model capabilities through vector operations by leveraging weighted combinations of task-specific knowledge. Given a base model with weights θ_{pre} and task-specific fine-tuned weights $\{\theta_t^{\text{ft}}\}_{t=1}^n$, task vectors are defined as:

$$\tau_t = \theta_t^{\text{ft}} - \theta_{\text{pre}} \quad (4)$$

The merged weights are then computed through:

$$\theta_{\text{Merge}} = \theta_{\text{pre}} + \lambda \sum_{t=1}^n \tau_t \quad (5)$$

where λ controls the magnitude of task-specific adaptations.

TIES-Merging is a parameter conflict resolution approach that operates in three stages. First, select the top $k\%$ parameters by magnitude of each task vector τ_t :

$$\hat{\tau}_t = \text{TopK}(\tau_t, k) \quad (6)$$

Next, Generating a consensus sign vector by examining the aggregate direction of parameter changes across all tasks:

$$\hat{\gamma} = \text{sgn} \left(\sum_{t=1}^n \hat{\tau}_t \right) \quad (7)$$

Finally, computing the average update magnitude considering only those task vectors whose signs align with the consensus direction:

$$\tilde{\tau} = \text{Average}(\{\hat{\tau}_t : \text{sgn}(\hat{\tau}_t) = \hat{\gamma}\}) \quad (8)$$

The final merged model weights are then computed as:

$$\theta_{\text{Merge}} = \theta_{\text{pre}} + \lambda * \tilde{\tau} \quad (9)$$

SLERP (Spherical Linear Interpolation) computes optimal geodesic paths between model weights through:

$$\text{SLERP}(\theta_1, \theta_2, t) = \frac{\sin((1-t)\omega)}{\sin(\omega)} \theta_1 + \frac{\sin(t\omega)}{\sin(\omega)} \theta_2 \quad (10)$$

where $\omega = \arccos \left(\frac{\langle \theta_1, \theta_2 \rangle}{\|\theta_1\| \|\theta_2\|} \right)$ and $t \in [0, 1]$ is the interpolation parameter.

Linear Merging implements straightforward weighted averaging:

$$\theta_{\text{Linear}} = \sum_{t=1}^n w_t \theta_t \tag{11}$$

where $\sum_{t=1}^n w_t = 1$ and $w_t \geq 0$.

A.3. Descriptions of SMAC-based Multi-Fidelity Optimization

Our implementation builds upon SMAC (Lindauer et al., 2022), which combines Hyperband (HB) (Li et al., 2018) and Bayesian Optimization (BO) (Snoek et al., 2012), utilizing Random Forest (Breiman, 2001) as the surrogate model. Let b_{max} and b_{min} denote the maximum and minimum budgets respectively, and $\eta > 1$ be a budget spacing parameter. SMAC determines $s_{\text{max}} = \lfloor \log_{\eta}(R) \rfloor$ brackets. Each bracket i begins with $n_i = \lfloor \eta^{s_{\text{max}} - i} \cdot \frac{\eta}{\eta - 1} \rfloor$ configurations and executes Successive Halving across $\lfloor \log_{\eta}(\frac{n_i}{n_{\text{min}}}) \rfloor + 1$ rounds. Each round evaluates all configurations with budget b , retains the top $\lfloor \frac{n_i}{\eta^l} \rfloor$ performers, and increases their budget to ηb for the next round, where l denotes the current round. This process continues until reaching either a single configuration or b_{max} . The Random Forest model incorporates configuration-performance pairs from previous evaluations, updating before each Successive Halving iteration using evaluations from all budget levels while prioritizing data from the largest available budget. The model guides configuration selection through Expected Improvement, enabling efficient exploration while maintaining evaluation quality. As optimization progresses, more configurations undergo evaluation at higher budgets, allowing the model to overcome potential misguided conclusions from lower-fidelity evaluations by ultimately relying on high-fidelity results. This integration of Hyperband’s resource allocation with Bayesian optimization’s surrogate modeling enables efficient exploration of the configuration space while maintaining evaluation quality through principled multi-fidelity optimization.

A.4. Details of Datasets Information

For searching, We use data from three reasoning domains: 1,000 GSMPlus (Li et al., 2024) samples, an adversarial variant of GSM8K with mathematical perturbations for testing math reasoning; 300 MBPP (Austin et al., 2021) samples (200 training/100 validation) for code understanding; and 700 samples from MMLU validation (Hendrycks et al., 2020) for general reasoning. These datasets support both single-objective optimization when used separately and multi-objective optimization when combined. For comprehensive performance evaluation, we employ established benchmark test sets across three key domains: mathematical reasoning using the complete test sets from GSM8K (Cobbe et al., 2021) and MATH (Hendrycks et al., 2021), code generation using the standard test splits from MBPP (Austin et al., 2021) and HumanEval (Chen et al., 2021), and general knowledge using the MMLU test set (Hendrycks et al., 2020), which spans diverse knowledge domains.

A.5. Evaluation Metrics and details

We evaluate using domain-specific metrics: accuracy for MMLU multiple choice questions based on loglikelihood, zero-shot accuracy for GSM8K and MATH, and Pass@1 for HumanEval and MBPP. We run all evaluations using LM Evaluation Harness (Gao et al., 2024) with vLLM (Kwon et al., 2023) acceleration. For consistency, we use fixed parameters across all tests: batch size 16, temperature 0.0 for greedy decoding, and maximum generation length of 1,024 tokens for GSM8K and 2,048 tokens for other datasets. All experiments run on NVIDIA Tesla A100 GPUs.

A.6. Details of Search Spaces

Within LFS, we define specific parameter ranges for each merging method: Task Arithmetic utilizes task vector weights $\lambda \in [0, 1]$; TIES-Merging combines task vector weights $\lambda \in [0, 1]$ with a ratio to retain parameters $k \in [0.1, 0.99]$; Linear-merging optimizes model coefficients $w_t \in [0, 1]$ subject to $\sum_i w_t = 1$; and Slerp employs an interpolation parameter $t \in [0, 1]$.

Table 8. Search Ranges of Hyperparameters for Different Model Merging Methods

Model Merging Methods	Search Ranges of Hyperparameters
Task Arithmetic	Scaling term to merge parameters: [0.5, 1.0]
Linear Merging	Scaling term to merge parameters: $[1/n]$ (n : number of models)
TIES-Merging	Scaling term to merge parameters: [0.5, 1.0] Ratio to retain parameters with largest-magnitude values: [0.5, 0.7, 0.9]

A.7. Details of Grid Search on Hyperparameters of base Model Merging Methods

A.8. Details of search on other Reasoning Tasks

LogiQA is derived from the logical comprehension section of China’s National Civil Servants Examination, specifically designed to evaluate candidates’ critical thinking and problem-solving capabilities. For our search implementation, we utilize the validation dataset with a budget range of 100 – 651.

OpenBookQA is used to measure deep understanding of both subject matter and language comprehension. The dataset comes with an "open book" of fundamental facts. We conducted experiments both with and without facts in the prompt. Our search employs the validation dataset with a budget range of 100 – 500.

PIQA (Physical Interaction: Question Answering) serves as a benchmark dataset for physical commonsense reasoning, with a particular focus on everyday situations and unconventional solutions. We have sampled 1,000 examples from the validation dataset for our search purposes, setting the budget range at 100 – 1,000.

SocialIQA stands as a comprehensive benchmark for testing social commonsense intelligence, this dataset evaluates understanding of human actions and their social implications in everyday situations. Our search implementation uses a 1,000-sample subset from the validation data, with a budget range of 100 – 1,000.

MGSM (Multilingual Grade School Math Benchmark) is a benchmark of grade-school math problems. The same 250 problems from GSM8K are each translated via human annotators in 10 languages. We use 1,069 mathematics problems and solutions translated to Japanese from the GSM8K test set by Sakana AI for searching, set a budget range of 100 – 1000.

B. Additional Experimental Results.

B.1. Detailed breakdown of performance across specific MMLU categories of GEN-DIS-0 and GEN-DIS-1

Table 9. Performance Comparison on MMLU Subject Categories between LM and GEN-DIS

MMLU Category	LM	GEN-DIS-0	GEN-DIS-1
Social Sciences	62.24	63.24 (+1.00)	63.69 (+1.45)
Humanities	49.52	51.31 (+1.79)	51.09 (+1.57)
STEM	42.82	43.67 (+0.85)	44.37 (+1.55)
Other	61.31	62.66 (+1.35)	62.12 (+0.81)

B.2. Additional result of Budget Distribution

Table 10. Budget Distribution Across Models

Budget	MATH-LFS	CODE-LFS	Multi-LFS	GEN-LFS	GEN-DIS-0	GEN-DIS-1
100	263 (47.2%)	295 (59.0%)	240 (48.0%)	207 (41.4%)	163 (16.3%)	311 (31.1%)
300	152 (30.4%)	205 (41.0%)	161 (32.2%)	181 (36.2%)	165 (16.5%)	307 (30.7%)
1000	85 (17.0%)	-	99 (19.8%)	112 (22.4%)	109 (10.9%)	186 (18.6%)
0	-	-	-	-	563 (56.3%)	196 (19.6%)

Table 11. Configuration parameters of architectures Searched by LFS

Group	Method	Metric	MATH-LFS	GEN-LFS	MULTI-LFS-0	MULTI-LFS-1	MULTI-LFS-2	MULTI-LFS-3	MULTI-LFS-4
Group (1-10)	task_arithmetic	mip	0.983	-	-	0.303	0.303	0.303	0.293
		att	0.182	-	-	0.948	0.948	0.948	0.881
		other	0.791	-	-	0.997	0.997	0.997	0.997
linear	mip	-	[0.118, 0.324, 0.558]	[0.351, 0.344, 0.304]	-	-	-	-	-
	att	-	[0.430, 0.224, 0.346]	[0.162, 0.298, 0.540]	-	-	-	-	-
	other	-	[0.317, 0.257, 0.426]	[0.288, 0.371, 0.340]	-	-	-	-	-
Group (11-20)	task_arithmetic	mip	0.982	-	0.395	0.395	0.395	0.395	0.395
		att	0.604	-	0.842	0.842	0.842	0.842	0.862
		other	0.329	-	0.300	0.300	0.300	0.300	0.300
linear	mip	-	[0.376, 0.258, 0.366]	-	-	-	-	-	-
	att	-	[0.414, 0.357, 0.229]	-	-	-	-	-	-
	other	-	[0.263, 0.532, 0.205]	-	-	-	-	-	-
sleep(Math, Code)	mip	0.594	-	-	-	-	-	-	-
	att	0.566	-	-	-	-	-	-	-
	other	0.323	-	-	-	-	-	-	-
Group (21-30)	ties	mip	-	-	0.778/0.583	0.778/0.583	0.819/0.583	-	0.724/0.583
		att	-	-	0.394/0.312	0.394/0.312	0.373/0.312	-	0.488/0.312
		other	-	-	0.324/0.606	0.349/0.606	0.324/0.606	-	0.371/0.606
linear	mip	-	-	-	-	-	[0.4739, 0.4728, 0.0533]	-	-
	att	-	-	-	-	-	[0.3916, 0.3649, 0.2435]	-	-
	other	-	-	-	-	-	[0.0342, 0.2826, 0.6832]	-	-
sleep(LM, Math)	mip	0.469	-	-	-	-	0.113	-	-
	att	0.437	-	-	-	-	0.339	-	-
	other	0.549	-	-	-	-	0.58	-	-
Group (31-40)	linear	mip	-	-	[0.354, 0.382, 0.264]	[0.375, 0.392, 0.234]	-	[0.373, 0.390, 0.237]	[0.354, 0.382, 0.264]
		att	-	-	[0.568, 0.141, 0.292]	[0.556, 0.168, 0.276]	-	[0.562, 0.159, 0.279]	[0.548, 0.156, 0.296]
		other	-	-	[0.344, 0.183, 0.473]	[0.345, 0.183, 0.473]	-	[0.345, 0.183, 0.473]	[0.345, 0.183, 0.473]

Table 12. DIS-Optimized Architecture Parameters for General Reasoning

block	GEN-DIS-0				GEN-DIS-1			GEN-DIS-NR		
	layer_0	layer_1	layer_2	scale	layer_0	layer_1	scale	layer_0	layer_1	scale
1	LM	-	-	1.00	LM	-	0.99	LM	-	1.07
2	Math	-	-	1.00	Base	-	0.78	LM	-	1.00
3	LM	-	-	1.00	LM	-	0.93	LM	-	1.00
4	LM	-	-	1.00	LM	-	1.01	LM	-	1.00
5	LM	-	-	1.00	LM	-	1.00	LM	-	1.00
6	LM	-	-	1.00	LM	-	0.93	LM	-	1.00
7	LM	-	-	1.00	Base	-	1.10	LM	-	1.00
8	LM	-	-	1.00	LM	-	1.00	LM	-	1.00
9	LM	-	-	1.00	LM	-	1.14	LM	-	1.00
10	LM	-	-	1.01	LM	-	1.00	LM	-	1.00
11	LM	-	-	1.00	Base	-	1.00	LM	-	0.97
12	Code	-	-	1.00	LM	-	0.95	LM	-	1.00
13	LM	-	-	1.00	LM	-	0.99	LM	-	1.12
14	LM	-	-	1.00	LM	-	1.00	LM	-	1.00
15	LM	-	-	1.00	LM	-	0.92	LM	-	1.14
16	LM	-	-	1.07	LM	-	0.89	LM	-	0.89
17	LM	-	-	1.00	Base	-	1.00	LM	-	1.00
18	Code	LM	-	1.00	LM	LM	1.00	LM	-	1.00
19	LM	-	-	1.00	LM	LM	1.00	LM	-	1.00
20	Code	-	-	1.00	LM	-	1.00	LM	-	1.00
21	Base	-	-	1.00	Base	-	1.00	-	-	1.15
22	LM	-	-	1.00	LM	-	1.00	LM	-	1.00
23	Math	LM	-	1.00	LM	-	1.00	LM	-	1.04
24	Base	-	-	1.00	LM	LM	1.00	LM	-	1.00
25	Code	LM	-	1.00	LM	-	1.00	-	-	1.00
26	Base	-	-	1.00	LM	-	1.00	-	-	0.93
27	Base	-	-	1.05	LM	-	1.05	LM	-	1.00
28	Math	LM	-	1.00	LM	LM	1.00	LM	LM	1.06
29	LM	-	-	1.07	LM	-	1.00	LM	-	1.00
30	Math	LM	-	0.87	LM	LM	1.00	LM	-	1.21
31	Base	-	-	1.00	LM	LM	1.00	LM	LM	1.00
32	Math	LM	-	1.00	LM	-	1.05	LM	-	1.10
33	LM	-	-	1.00	Base	-	1.00	LM	LM	0.99
34	LM	-	-	1.00	LM	LM	1.00	LM	-	1.00
35	LM	-	-	1.00	LM	-	1.00	LM	-	1.08
36	LM	-	-	1.20	Base	-	1.00	LM	-	1.07
37	Base	-	-	1.00	LM	-	1.13	LM	LM	1.32
38	Code	-	-	1.00	LM	-	1.03	LM	LM	1.00
39	Math	LM	-	1.00	LM	-	1.00	LM	-	1.00
40	Code	-	-	1.00	LM	-	1.01	LM	-	1.00

Table 13. DIS-Optimized Architecture Parameters for OpenbookQA

block	OpenbookQA				OpenbookQA+F			
	layer_0	layer_1	layer_2	scale	layer_0	layer_1	layer_2	scale
1	LM	-	-	1.00	Base	-	-	0.96
2	Code	-	-	1.00	Code	LM	-	1.00
3	LM	-	-	1.00	LM	-	-	1.00
4	LM	-	-	1.00	LM	-	-	0.97
5	LM	-	-	1.06	LM	Code	-	1.00
6	LM	-	-	1.00	Base	-	-	1.00
7	LM	-	-	1.00	Base	-	-	1.00
8	Math	LM	-	1.00	LM	-	-	1.19
9	LM	-	-	1.00	Code	-	-	1.00
10	LM	-	-	1.00	LM	-	-	1.00
11	LM	-	-	1.00	Math	-	-	1.00
12	Base	-	-	1.00	Base	-	-	1.00
13	LM	-	-	1.00	LM	-	-	0.91
14	LM	-	-	1.00	Base	-	-	1.00
15	LM	-	-	1.00	LM	-	-	1.08
16	LM	-	-	1.00	LM	-	-	1.00
17	LM	-	-	1.00	LM	-	-	0.99
18	LM	-	-	0.85	LM	-	-	1.00
19	LM	-	-	1.00	LM	-	-	1.00
20	LM	-	-	1.00	Code	-	-	1.07
21	LM	-	-	1.00	Base	-	-	1.21
22	LM	-	-	1.00	LM	-	-	0.98
23	LM	-	-	1.00	Code	-	-	1.00
24	LM	-	-	1.00	Base	-	-	0.92
25	Code	LM	-	1.00	LM	-	-	1.00
26	Base	-	-	1.00	LM	-	-	0.93
27	Code	LM	-	1.00	Math	LM	-	1.08
28	Code	LM	-	0.96	Code	-	-	1.18
29	LM	-	-	1.00	LM	-	-	1.00
30	Math	LM	-	1.00	Code	LM	-	1.01
31	LM	-	-	1.00	LM	-	-	0.89
32	LM	-	-	1.00	Base	-	-	1.05
33	LM	-	-	1.00	LM	-	-	1.00
34	LM	-	-	1.00	Math	LM	-	0.83
35	LM	-	-	1.00	Code	LM	-	1.12
36	LM	-	-	1.20	LM	-	-	1.00
37	LM	-	-	1.00	Math	-	-	1.13
38	LM	-	-	1.00	LM	-	-	1.03
39	LM	-	-	1.00	Math	-	-	1.00
40	LM	-	-	1.00	Base	-	-	1.01

Table 14. DIS-Optimized Architecture Parameters for MGSM_JA

block	MGSM_JA_0				MGSM_JA_1		
	layer_0	layer_1	layer_2	scale	layer_0	layer_1	scale
1	Base	-	-	0.99	Math	-	0.98
2	Math	-	-	1.00	Base	-	1.12
3	Math	-	-	0.96	LM_JA	-	1.00
4	Math	-	-	1.00	Base	-	1.00
5	Math	-	-	1.00	Math	LM_JA	1.00
6	Math	-	-	1.00	Math	-	0.93
7	Math	LM	-	1.00	Math	-	1.00
8	Math	-	-	1.11	Math	-	1.00
9	Math	LM	-	1.00	Math	-	1.00
10	Math	-	-	1.10	Math	LM_JA	1.00
11	Math	-	-	1.00	LM_JA	-	1.00
12	Math	LM	-	1.06	Math	LM_JA	1.00
13	LM	Math	-	1.00	Math	-	1.00
14	LM	Math	-	0.83	Math	-	0.97
15	Math	-	-	0.86	Base	-	1.00
16	Math	-	-	1.00	Base	-	0.99
17	Code	-	-	1.00	Math	-	1.09
18	Math	-	-	1.00	Math	-	1.00
19	Base	-	-	1.00	Base	-	0.90
20	Math	-	-	1.00	Math	-	1.26
21	Base	-	-	1.00	Base	-	1.24
22	Base	-	-	1.00	Base	-	1.00
23	Math	-	-	0.96	Math	-	0.82
24	Base	-	-	0.85	Math	-	1.08
25	Math	-	-	1.01	Base	-	1.00
26	Code	-	-	1.00	Base	-	1.00
27	Math	-	-	1.00	LM_JA	-	1.00
28	Math	-	-	1.00	Math	-	1.07
29	Math	-	-	1.00	Base	-	1.00
30	Base	-	-	1.00	LM_JA	Math	0.87
31	Code	-	-	1.04	Math	LM_JA	0.84
32	Math	LM	-	0.89	Math	LM_JA	0.99
33	Math	-	-	1.00	Math	-	1.00
34	Base	-	-	1.00	Math	LM_JA	0.73
35	LM	-	-	1.00	Math	-	1.00
36	Math	-	-	0.98	LM_JA	-	1.00
37	Math	-	-	1.00	Math	-	1.00
38	Base	-	-	1.00	Math	LM_JA	1.00
39	Math	-	-	0.95	Math	-	1.00
40	Base	-	-	1.00	Math	-	1.00